Use of a bottom-mounted hydroacoustic sonar to assess fish presence and vertical distribution at the FORCE in-stream tidal turbine test site in Minas Passage

Final Report

to the

Offshore Energy Research Association of Nova Scotia

Submitted
by
Haley Viehman and Anna Redden
Acadia Centre for Estuarine Research
Acadia University

February 2018

ACADIA ESTUARINE CENTRE FOR RESEARCH

Executive summary

The effects on fish of large tidal in-stream energy conversion (TISEC) devices deployed in very high flow environments (>2 m/s) are generally unknown. This uncertainty is concerning to regulators, scientists, and other stakeholders of the marine environment (e.g., fishers), particularly in areas where species of special concern (e.g. endangered, threatened, or commercial) are present. To help address these concerns, FORCE developed the Fundy Advanced Sensor Technology (FAST) platforms, equipped with sensors to monitor physical and biological characteristics of the FORCE test area. The first deployment of a FAST platform at the FORCE site occurred from December 2015 to January 2016, and it included an upward-facing echosounder, the ASL Acoustic Zooplankton and Fish Profiler (AZFP).

To better understand fish use of this site and their potential for interaction with TISEC devices, we examined how fish density and vertical distribution (measured by the AZFP) varied with respect to environmental factors, in particular tidal stage and time of day, and how these factors influence spatial overlap of fish with a TISEC device. The TISEC device considered here was the Cape Sharp Tidal (CST) device (OpenHydro design), which was later deployed at the FORCE site from November 2016 to June 2017.

The AZFP echosounder was found to perform well in the FORCE high-flow environment. All AZFP data were processed in Echoview® software to remove non-target hydroacoustic backscatter, most of which was from entrained air. This resulted in omission of the upper 10 m of the water column from analysis. Cleaned data were subsequently split into time-depth cells, echo-integrated, and exported for statistical analysis. The processing steps and templates created for this project can be applied to future AZFP data collected with the FAST platform.

The presence (relative density) and vertical distribution of fish were examined with respect to tidal and diel stages. We found that fish were almost constantly present during the data collection period, with higher densities during the flood tide than the ebb tide. Fish density was highest in the upper portion of the water column analyzed (above 15-20 m from the sea floor), though fish were more evenly spread throughout the water column at night than during the day. Species of fish could not be determined from the acoustic data, so we recommend using multiple acoustic frequencies in the future, alongside general knowledge of which species are in the area during data collection periods (e.g., by drawing on local knowledge of the fish species present, their migration timing, and their behaviors).

The observed vertical distributions of fish were used to generate basic spatial overlap probability models, which estimated the probability that fish within the passage cross-section might spatially overlap with (and therefore potentially encounter) a TISEC device under different vertical distribution scenarios. While there were apparent differences in the vertical distribution of fish in relation to tidal stage (e.g. from ebb to flood tide), the estimated overlap probabilities for a single TISEC device were very low (< 0.002). Spatial overlap probabilities, however, may become important for arrays of devices. The determination of encounter probability will require additional information, including a determination of the probability that a fish (preferably of known species) will pass through the Minas Passage during some defined time interval. Hydroacoustic data on the horizontal distribution of fish (across the Minas Passage), as well as data on nearfield fish behavior in response to TISEC devices in high-flow environments, would also aid the development of models of in-stream turbine effects on fish.

Contents

1 Introduction

The effects on fish of large tidal in-stream energy conversion (TISEC) devices deployed in very high flow environments (>2 m/s) are generally unknown. This uncertainty is of interest to regulators, scientists, and other stakeholders of the marine environment (e.g., fishers), particularly in areas where species of special concern (e.g. endangered, threatened, or commercial) are present. Direct contact of fish with turbine blades and indirect effects on behaviour (such as use of natural migratory pathways) continue to be the primary concerns.

To help address the environmental monitoring challenges faced by TISEC developers at the Fundy Ocean Research Center for Energy (FORCE) test site, FORCE developed the Fundy Advanced Sensor Technology (FAST) platforms: cabled and non-cabled platforms equipped with sensors to monitor physical and biological characteristics of the FORCE test area. The first deployment of a FAST platform in the FORCE test area occurred in December 2015, and it included an upward-facing echosounder (ASL Acoustic Zooplankton and Fish Profiler, or AZFP). This successful deployment is the first long-term (4 weeks), active acoustic monitoring of fish presence and vertical distribution in Minas Passage. Such deployments are planned to occur several times per year through 2018. These acoustic data can help us understand how fish naturally use the FORCE test site, and therefore inform predictions of the likelihood of fish encountering TISEC devices in the future.

The following report details the analysis of this first 4-week acoustic dataset (December 2015 – January 2016) collected from the FAST platform. We examined how fish density and vertical distribution varied with respect to environmental factors such as tidal stage and time of day, and how these could influence probability of spatial overlap, and ultimately encounter probability, with a TISEC device. The TISEC device considered in this report was the Cape Sharp Tidal (CST) device (OpenHydro design), which was deployed at the FORCE site from November 2016 to June 2017. We also assessed the performance capabilities of the upward facing AZFP (mounted to the FAST sensor platform) at the FORCE test site as a means to inform future deployments and sensor arrangements on the FAST platform and potentially other structures (e.g. turbine infrastructure) installed in Minas Passage.

2 Methods

2.1 Data collection

Hydroacoustic data were collected with an upward-facing ASL Environmental Sciences Acoustic Zooplankton and Fish Profiler (AZFP), mounted approximately 1.5 m above the sea floor on the FAST-1 platform (Figure 1).

Figure 1. FAST-1 sensor platform developed by FORCE and deployed at the FORCE test site from 8 December 2015 to 5 January 2016. White arrow indicates location of AZFP transducer. Photo credit: Tyler Boucher.

The AZFP continuously operated a 125 kHz, 8° (half-power beam angle) circular transducer, which operated at a 300 μs pulse duration and a ping rate of 1 Hz. Current velocity and water temperature were recorded for 10 minutes every half hour by a Nortek Signature 500 Acoustic Doppler Current Profiler (ADCP), also mounted on the platform. The platform was deployed at the south-west corner of the FORCE test site from 8 December 2015 to 5 January 2016 (Figure 2). This site is on a volcanic plateau formation that extends into Minas Passage, the 5.5-km-wide connection between Minas Basin and Minas Channel. Mid-water-column current speed at the platform's location exceeded 4 m·s^{-1} at peak flood tide and 3 m·s^{-1} at peak ebb tide, depth ranged from 33 m to 45 m during the spring tide, and temperatures ranged from 5.4°C to 8.4°C. The CST device considered in this project was deployed at Berth D (Figure 2) in November 2016 (after data collection).
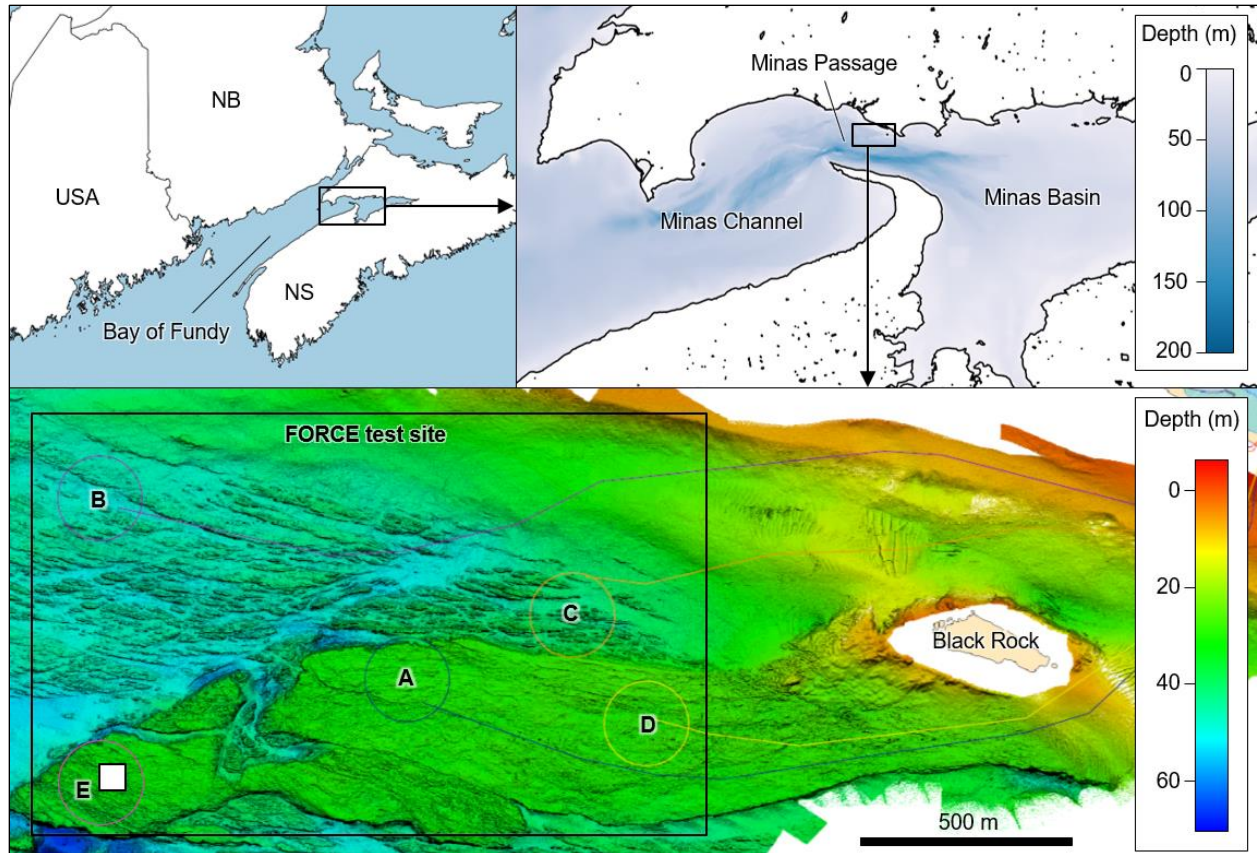
Figure 2. Study site with deployment location. Lower panel shows site bathymetry and proposed MHK device sites (A-D) at the FORCE test site. Location of the FAST-1 platform in December 2015 – January 2016 indicated by □. Upper panel maps made in QGIS with data obtained from GeoGratis Canada and bathymetry data from [1]. Lower panel map produced by Seaforth Geosurveys, Inc.

2.2 Data processing

Hydroacoustic data were processed using Echoview® software (8.0, Myriax, Hobart, Australia). This required many steps, considerable time, and much scrutiny. The first processing step was to apply calibration coefficients. Calibration of the echosounder was carried out by the manufacturer prior to the deployment using a standard tungsten-carbide calibration sphere, and it was found to be accurate to within 1 dB. Corrections to sound speed and absorption coefficients were calculated for this deployment period based on average temperature (7.3°C) and salinity (32 ppt) in this well-mixed region.

Remaining processing steps focused on the removal of non-target acoustic backscatter. A target strength threshold of -60 dB was first applied to the data to remove signal from non-fish organisms, such as zooplankton, and any fish less than a few cm in length [2-8]. Data in the acoustic nearfield (0 to 1.7 m range) were also omitted from analysis, and any data showing acoustic interference from the co-located ADCP were manually identified and excluded. Entrained air near the surface was the largest source of unwanted backscatter (Figure 3a), particularly during peak current speeds, as has been the case at other tidal energy sites [9-11]. This noise was removed using a series of functions in Echoview®, including a modified version of bottom-detection algorithm to find the lower limit of the entrained air (Figure 3a), a filter to expand this region slightly, and a mask to entirely remove the entrained air signal from the data

3

(Figure 3b). This method worked well, though some fish aggregations near the surface were partially or entirely excluded by proxy. Any fish within plumes of entrained air were not detectable, and at times large portions of the water column were rendered unusable by entrained air extending far below the surface (particularly during fast flows). Most of the upper 10 m of the water column were masked by the acoustic backscatter of entrained air. In order to compare fish density and vertical distribution over time, without varying amounts of data omission influencing results, the upper 10 m layer of the water column was systematically excluded from further analyses (Figure 3c). Any pings in which entrained air extended below 10 m depth were also removed (Figure 3c).

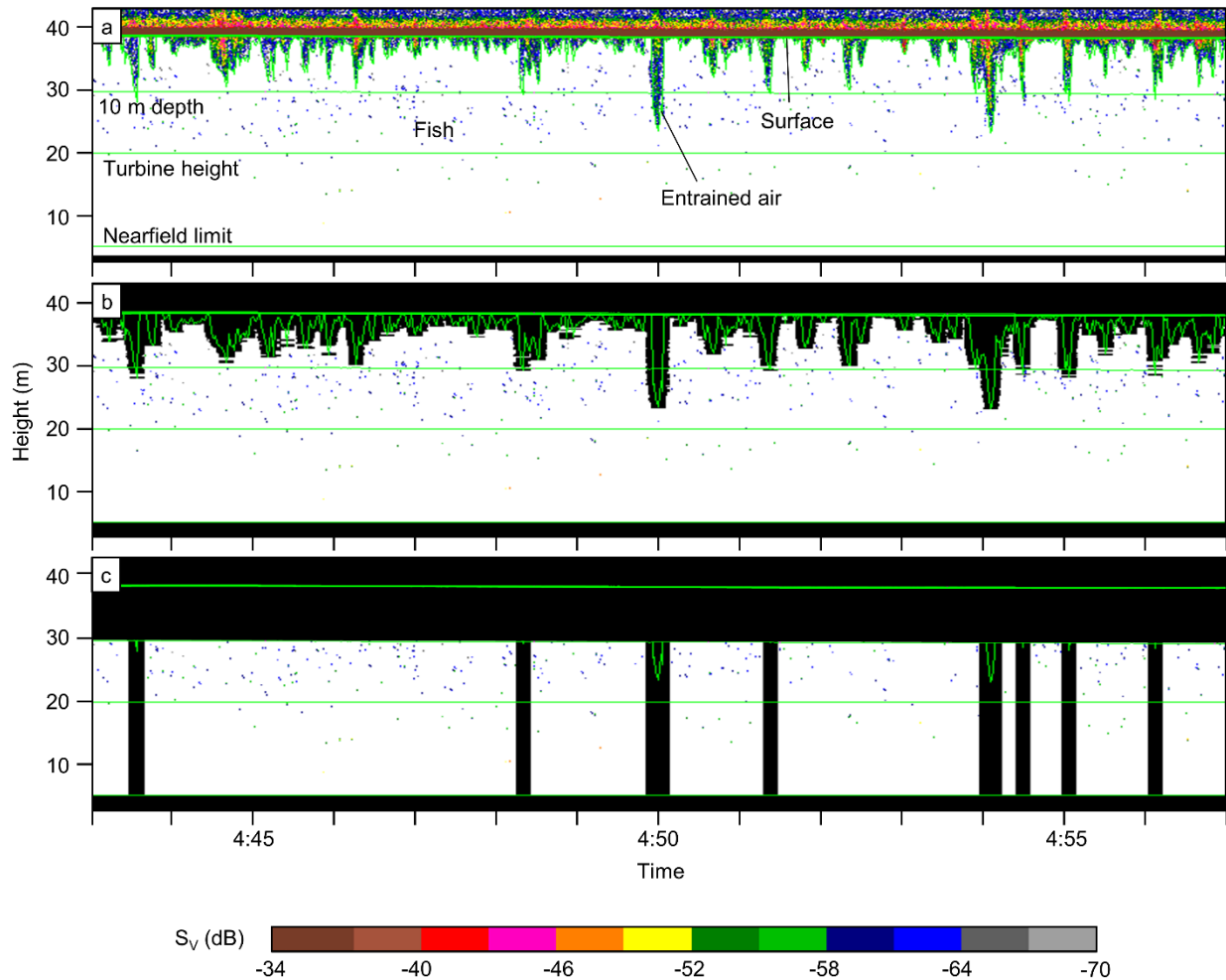

Figure 3. Example of volume backscatter (S_V) data collected from 4:43 to 4:57 UTC on 9 December 2015. (a) Raw data, showing entrained air and lines used in data processing. (b) Processed data, with entrained air removed. (c) Processed data with upper 10 m removed, as well as any data when depth of entrained air surpassed 10 m depth. Height is measured from the sea floor and time is in UTC.

2.3 Data analysis

Following data processing, analysis was divided into three parts: (1) analysis of fish backscatter (relative density) from the water column (Figure 4b), (2) inspection of the vertical distribution of backscatter (Figure 4c), and (3) comparison of backscatter from the depths spanned by the proposed TISEC device to backscatter from the water column (Figure 4d).
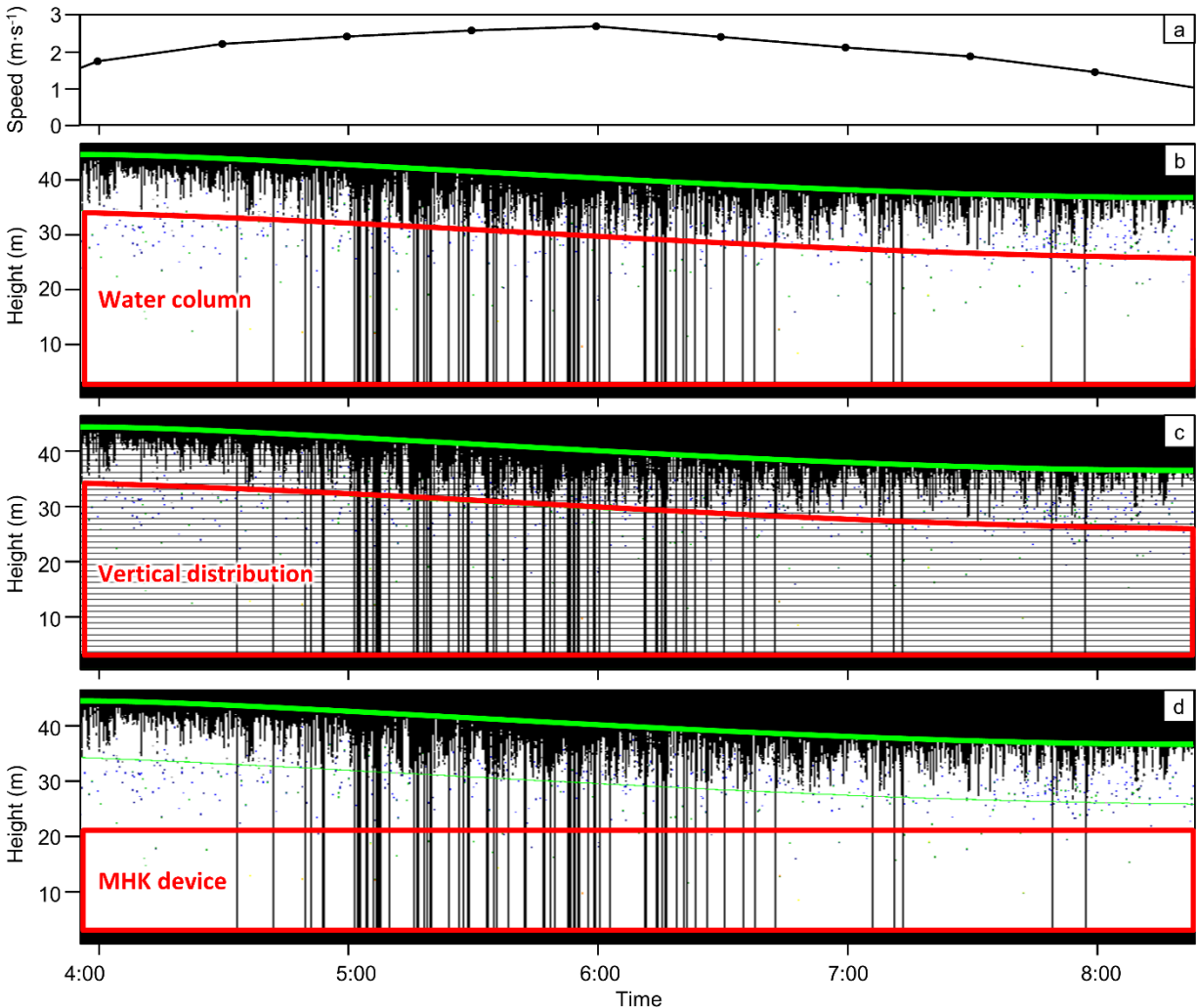

Figure 4. Data from one ebb tide from 3:56 to 8:23 UTC on 9 December 2015. (a) Current speed from 16-17 m above the sea floor. (b-d) The three water column partitions used in analysis: (b) entire water column, defined as the acoustic nearfield to the 10-m depth line; (c) 1-m layers for vertical distribution analysis; (d) layer that encompasses depths spanned by the TISEC device installed in November 2016. Height is measured upward from the sea floor, and time is in UTC. Vertical black lines are pings omitted due to entrained air (Figure 3c).

Hydroacoustic data were split into segments according to tidal (ebb or flood) and diel (day or night) stages. Slack tides were defined as periods when mid-water-column current speed was less than 1 m·s^{-1}. The rise and fall in current speed was slightly asymmetrical (Figure 4a), so low slack tide averaged 58.5 min (20.9 min standard deviation) in duration while high slack tide averaged 42.7 min (14.5 min standard deviation). Slack tides, approximately one hour long on average, were omitted from analyses in order to focus on ebb and flood tides, when a TISEC

5

device would be rotating (depending on cut-in speed) and therefore a potentially greater risk to fish. Periods of dusk and dawn were then defined as the hours centred at sunrise and sunset and were also excluded in order to avoid likely periods of vertical fish migration that could confound analysis of vertical distribution. The remaining data segments were classified by tidal stage and diel stage, and were treated as separate samples. Any of these samples missing more than half of their data points due to data processing steps were omitted from analyses.

Further analysis required partitioning the water column in three different ways (Figure 4). As previously explained, the water column used in analyses was limited to the portion between the acoustic nearfield (3.2 m height above the sea floor) and the 10-m depth line (Figure 4b). From here onward, "water column" refers to the portion of the true water column which we were able to analyze. Assessing the vertical distribution of backscatter required splitting this water column into 1-m-deep layers measured upward from the face of the transducer (Figure 4c). To compare TISEC device depth to the rest of the water column, the water column was also split at the TISEC device height (20 m above the seafloor; Figure 4d).

The acoustic metrics exported from these portions of the water column for each time segment were mean volume backscatter and the area backscattering coefficient. Volume backscatter, S_V, is the amount of acoustic energy scattered by a unit volume of water and is a rough proxy for fish density [12,13]. However, the relationship between S_V and fish density depends on the acoustic target strength of the individual fish sampled, which varies with species and life stage. It is therefore a complicated transformation in areas with a mixed fish assemblage, such as the Minas Passage [14]. We therefore use S_V only as a rough relative index of fish density, with the knowledge that changes in the fish assemblage over time could influence observed values. S_V is expressed logarithmically in units of decibels (dB re 1 m^{-1}), or in the linear domain as s_v ($s_v = 10^{S_V/10}$), with units of m$^2 \cdot$m^{-3}. Mean S_V was calculated for the entire water column to examine general differences in fish density with respect to tidal stage and diel stage. The area backscattering coefficient, s_a, is s_v integrated over a given layer of the water column (units of m$^2 \cdot$m^{-2}), and so is also a proxy of fish density. The s_a was used to calculate the proportion of acoustic backscatter contributed by each 1-m layer of water and from the depths spanned by the proposed TISEC device.

Statistical analyses of these metrics were carried out in R (3.3.1, R Core Team, Vienna, Austria). Differences in water column S_V and the proportion of backscatter from the TISEC device depths related to tidal stage (ebb or flood) or diel stage (day or night) were examined using analysis of variance (ANOVA) tests with a significance level of 0.05. Comparisons between factor groups found to have significant effects were carried out with Tukey-type multiple comparisons. Nonparametric versions of these tests (permutation ANOVA with 5,000 iterations, nonparametric Tukey-type comparisons) were used for water column S_V measurements, as these data did not meet the assumptions of normality. The linear form of S_V (s_v) was used in significance testing and to calculate summary statistics.

The probability that fish moving through the passage might spatially overlap with the proposed TISEC device was estimated under three fish distribution scenarios: (1) uniform vertical distribution; (2) ebb tide vertical distribution; and (3) flood tide vertical distribution. Fish horizontal distribution (across the breadth of the passage) was assumed uniform for this exploratory exercise. Additionally, the proportion of backscatter at turbine depth was assumed

6

equivalent to the proportion of fish at that depth range. That is, acoustic properties were assumed the same for all fish, which would be the case, for example, if all fish detected were the same species and of similar size. Under scenario 1, the probability of spatial overlap was simply the cross-sectional area of the turbine divided by that of the Minas Passage. For scenarios 2 and 3, the probability was the proportion of passage cross-section spanned by the turbine's width multiplied by the proportion of fish at turbine depth (the median proportion of backscatter from turbine depth) during ebb and flood tides, respectively. The passage cross-sectional area at site D (Figure 5) was estimated as 338,814 m^2 at mean tidal height, using bathymetry data in [1] and Quantum GIS open source software package (2.18.7, QGIS Development Team). The area of a single CST device (turbine plus gravity base) was approximated as 320 m^2 (16 m width x 20 m height), and the area of the vertical slice of the passage spanned by the turbine was 592 m^2 (16 m width x 37 m depth).
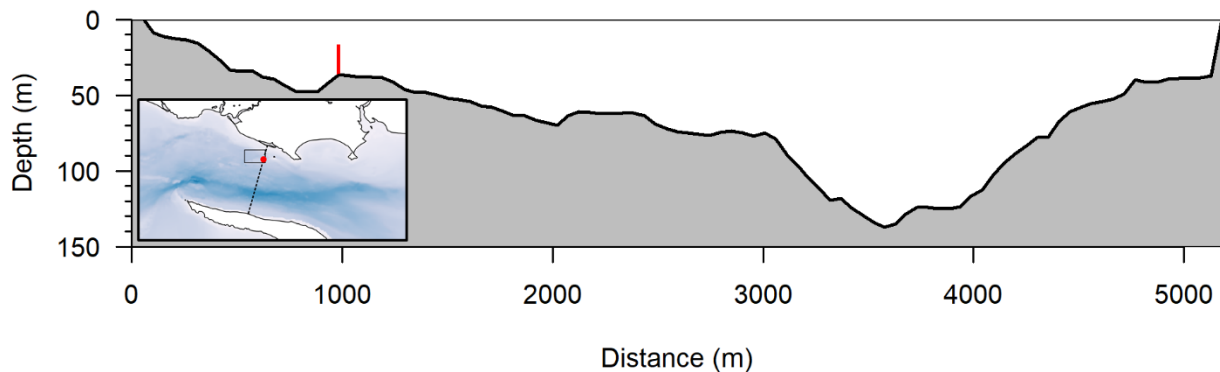

Figure 5. Cross-section of Minas Passage at TISEC device location. Red circle in inset map shows device location (Berth D, Figure 2) and dashed line indicates cross-section shown. Red rectangle in cross-section is the approximate area of the TISEC device. Bathymetry data from [1].

3   Results

From 8 December 2016 to 5 January 2016, approximately 16 GB of hydroacoustic data were collected by the AZFP housed on the FAST-1 platform. Visual scrutiny of all data collected (Figure 6, see page 12) indicated cyclic features of fish presence and vertical distribution. For example, low mid-water-column fish densities are apparent as light patches in the data (Figure 6) once per day in much of the dataset and are likely linked to the interaction of tidal and diel cycles.

After data processing, 51 flood tides and 64 ebb tides ocurring during either the day or night remained for use in analyses (Figure 7, see page 13). Fish were almost always present in the data. Individual fish spread throughout the water column as well as small, compact aggregations were present during the day, but no aggregations of fish were observed at night. During calm periods with little entrained air, fish could often be seen in the upper 10 m of water column that were excluded from analyses (Figures 3 and 4); such observations are important when interpreting results.

3.1 Water column fish density

The water column mean S_V (index of fish density) was significantly higher during the flood tide than the ebb tide by approximately 1 dB (median and IQR for ebb tide: -84.8 dB, -86.2 to -83.6; flood tide: -83.7 dB, -84.6 to -82.4; Figure 8b). Diel stage was not found to significantly affect water column mean S_V, though S_V was noticeably less variable at night than during the day (Figure 8a,c).
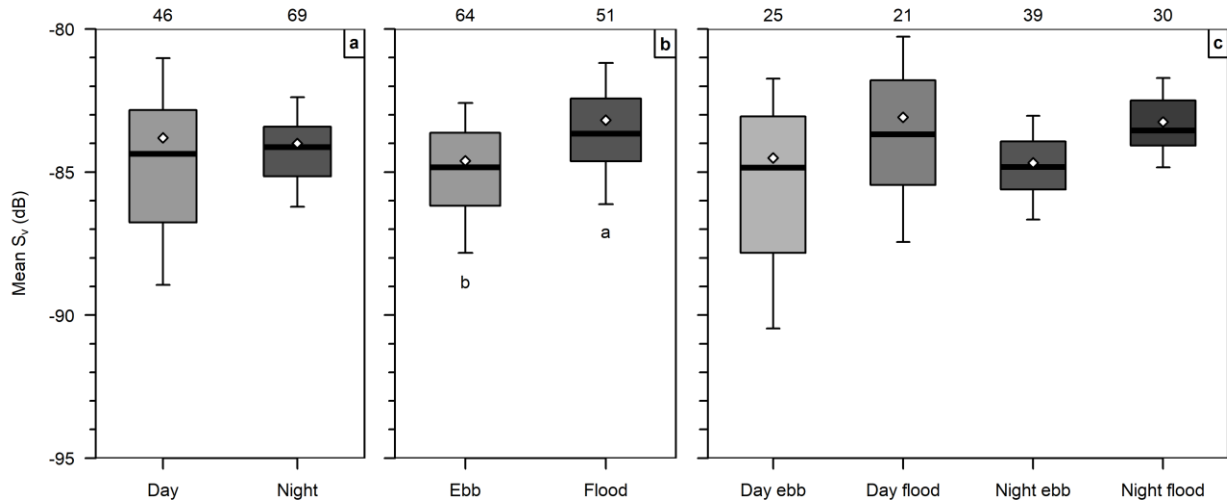

Figure 8. Water column mean volume backscatter, S_V (proportional to fish density), separated by (a) diel stage, (b) tidal stage, and (c) diel and tidal stage. Sample sizes shown at top, and letters indicate significantly different means (a highest, b lowest), where tested. White diamonds are means, horizontal bars are medians, boxes span 25th to 75th percentiles, and whiskers span 10th to 90th percentiles.

3.2 Vertical distribution

Vertical distributions were generally 'top-heavy' regardless of tidal stage or diel stage, with backscatter typically strongest in the upper layers analyzed (Figure 9). Differences in vertical distribution related to tidal and diel stage were also apparent. Diel differences were particularly noticeable: during the day (Figure 9a,c), backscatter was strongest in the upper layers of the water column, with a minimum centred at approximately 15 m above the sea floor. At night (Figure 9b,d), backscatter was distributed more evenly across depths, increasing from the lowest layers to approximately 20 m height above the sea floor. Tidal differences were confined to daytime, when vertical distribution was more variable during ebb tide than flood.
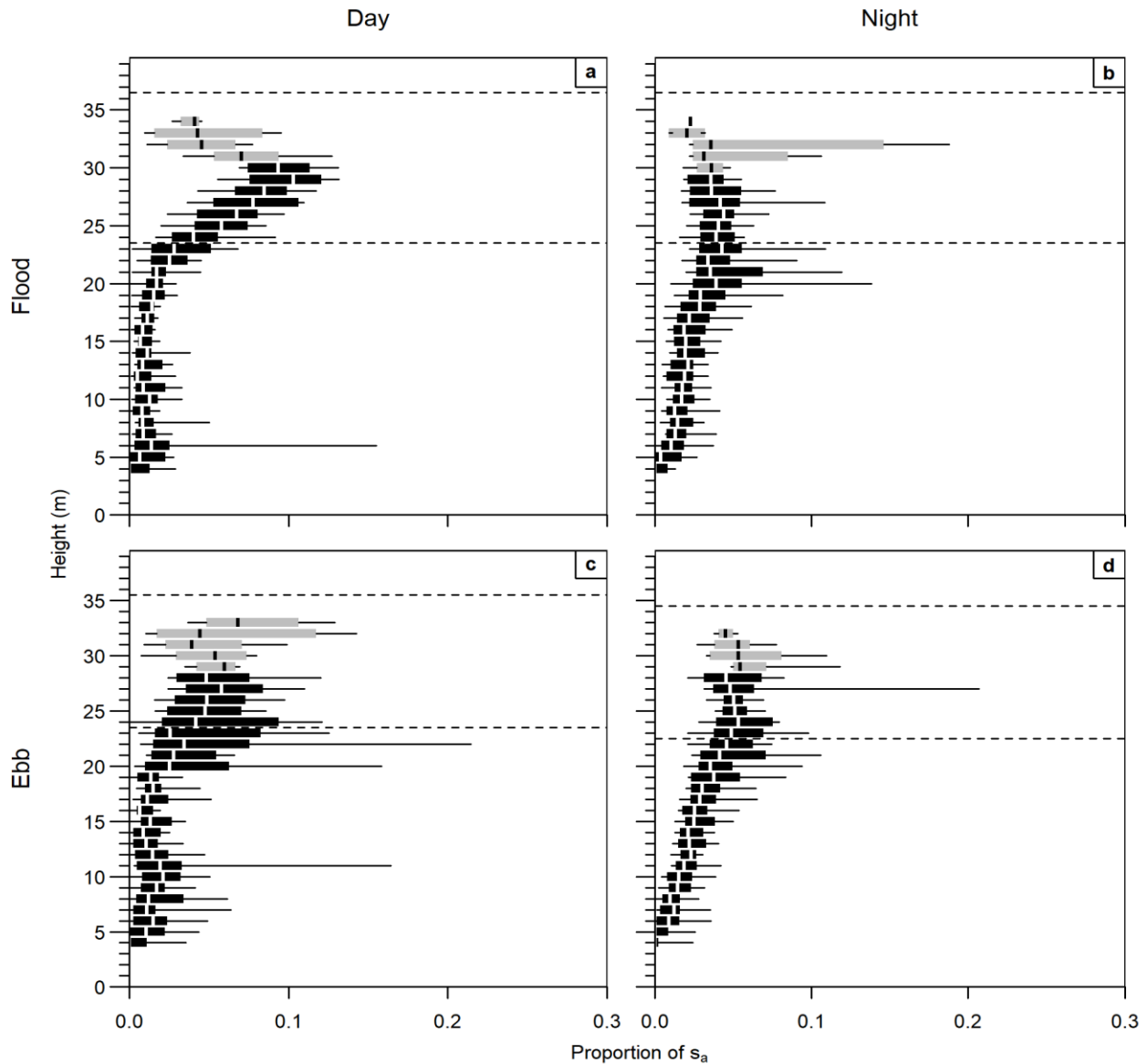
Figure 9. Vertical distribution of area backscatter separated by diel and tidal stages: (a) day flood, (b) night flood, (c) day ebb, (d) night ebb. Thick vertical lines indicate median, boxes encompass the interquartile range, and whiskers span the 10th to 90th percentiles of each 1-m layer of the water column. Grey boxes indicate sample sizes less than 10. Horizontal dashed lines are the minimum and maximum height of the analyzed water column (which extended from the seafloor to 10 m below the surface) for the duration of each time period plotted. Height is measured upward from the sea floor.

3.3 Fish at TISEC device depth

The proportion of fish backscatter from the depths spanned by the Cape Sharp Tidal TISEC device (0-20 m height) was significantly higher during the ebb tide than the flood tide (median, IQR for ebb: 0.401, 0.288-0.504; flood: 0.325, 0.202-0.451) (Figure 10). Diel stage did not significantly affect the proportion of backscatter within the device layer, despite visual differences in vertical distribution (Figure 9).
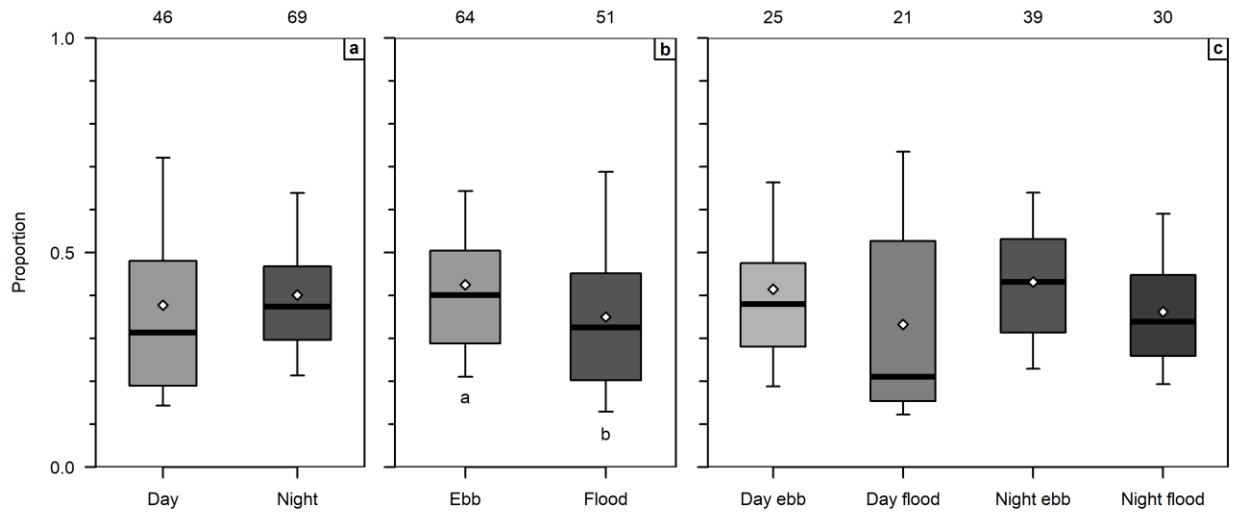
Figure 10. Proportion of water column area backscatter, s_a, from depths spanned by the proposed TISEC device (0-20 m above sea floor). Proportion separated by (a) diel stage, (b) tidal stage, and (c) diel and tidal stage. Sample sizes shown at top. Letters indicate groups with significantly different means (a highest, b lowest), where tested. White diamonds are means, horizontal bars are medians, boxes span 25th to 75th percentiles, and whiskers span 10th to 90th percentiles.

3.4 Probability of spatial overlap

The probability that fish would spatially overlap with the TISEC device, assuming uniform vertical and horizontal distribution of fish, was 0.00175. The probability of spatial overlap was 0.00070 with the observed ebb tide vertical distribution of fish (median proportion of fish at turbine depth = 0.401), and 0.00057 with the observed flood tide vertical distribution (median proportion of fish at turbine depth = 0.325).
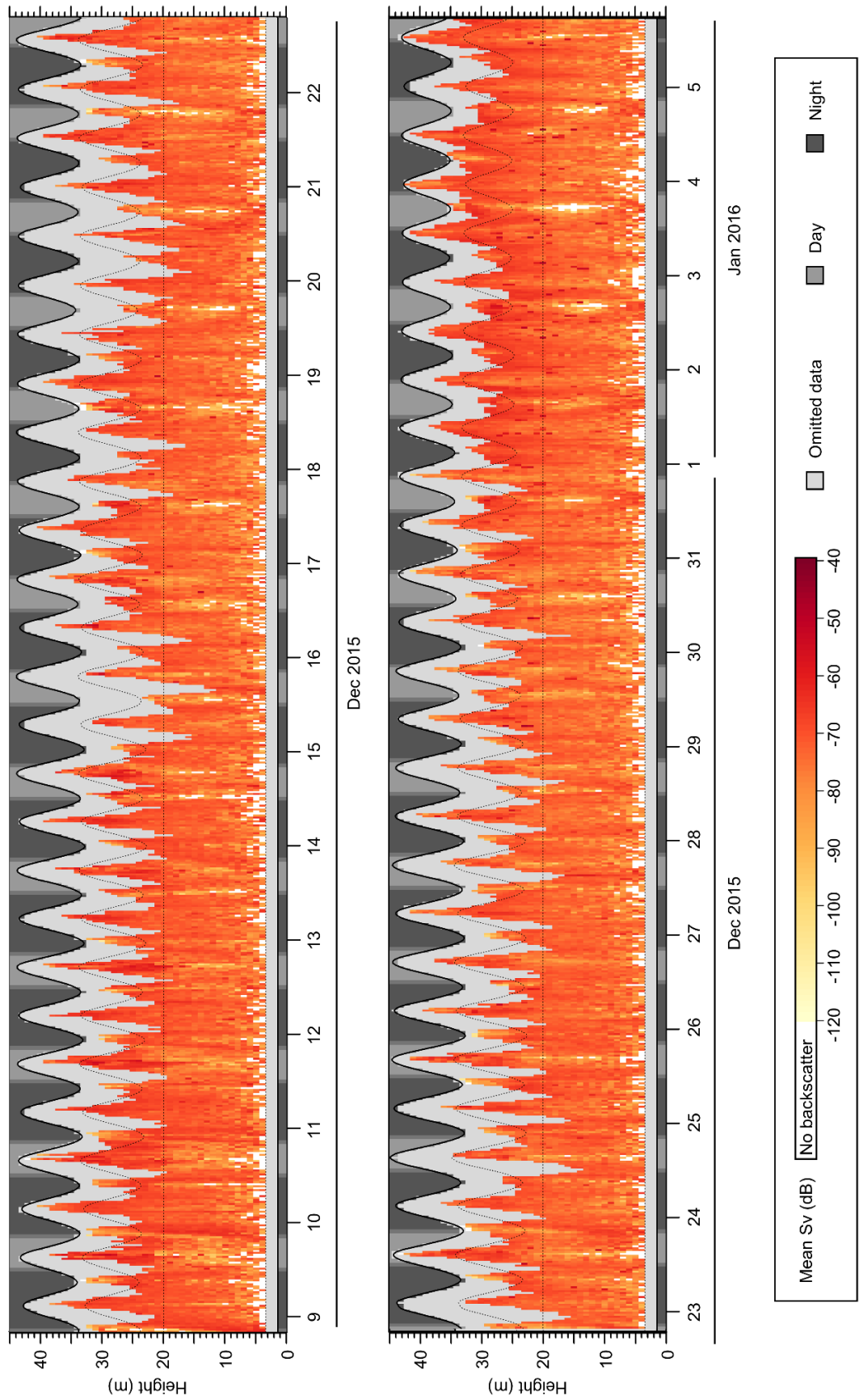
Figure 6. Summary of all mean volume backscatter (S$_V$) data collected from December 2015 to January 2016. Color indicates S$_V$ (index of fish density) for 1-m layers of the water column for each half-hour. White indicates no backscatter and darker, redder colors indicate higher S$_V$. Data omitted from analyses are in light gray. Day (medium gray), night (dark gray), and dusk and dawn are indicated in the background. Solid black lines are transducer and surface height. Dotted lines are the acoustic nearfield, height of the turbine, and 10-m depth. Height is measured upward from the sea floor and time is in UTC.
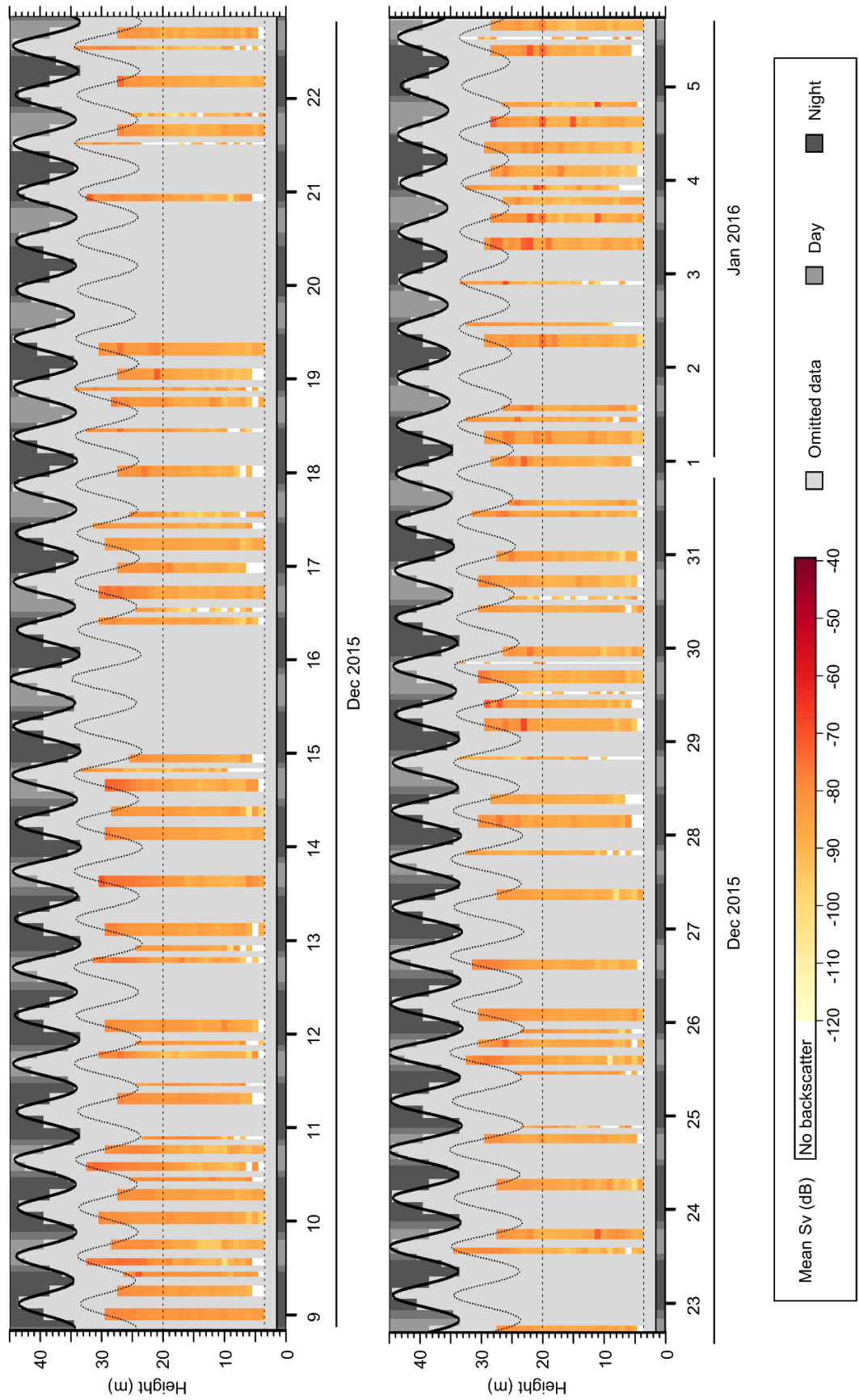
Figure 7. Summary of all mean volume backscatter (Sv) data used in analyses. Color indicates S_v (index of fish density) for 1-m layers of the water column for each time increment of interest (ebb and flood, day and night): white is no backscatter and darker, redder colors indicate higher S_v. Data omitted from analyses are in light gray. Day (medium gray), night (dark gray), and dusk and dawn are indicated in the background. Solid black lines are transducer and surface height. Dotted lines are the acoustic nearfield, height of the turbine, and 10-m depth. Height is measured upward from the sea floor and time is in UTC.

12

4 Discussion

4.1 Fish density and vertical distribution

Water column fish density and vertical distribution at FORCE was surprisingly consistent over the duration of the December-January dataset, and a later comparison found density to be higher than a similar data collection period that took place from June-July 2016 [15]. It is likely that most of the fish in the passage during data collection were Atlantic herring (*Clupea harengus*), the presence of which was supported by frequent trails of bubbles seen rising from schools or individuals in the echogram (herring and other clupeids are known to release swim bladder gas through the anal duct [16,17]). Rainbow smelt and sticklebacks were also potentially present in the area based on what is generally known of their life histories [18]. Acoustically tagged striped bass have been recorded repeatedly passing through Minas Passage with the tidal currents in the winter [19], indicating they were overwintering rather than migrating. It is possible this would also be the case for other fish species. Fish moving back and forth through the passage with the currents would result in more consistent backscatter over time, as opposed to the intermittent acoustic signal that would be expected from species passing through primarily in one direction, e.g. during migrations.

More information on the species of fish detected would aid our interpretation of acoustic data, as well as improve predictions of TISEC device effects on different fish populations. Species identification is always challenging when using active acoustics, but particularly when sampling mixed fish assemblages, such as in the Minas Passage [14, 18]. Species identification could be improved by using multiple acoustic frequencies [20, 21] alongside general knowledge of which species are in the area during data collection periods. The AZFP is capable of operating up to 4 single-beam transducers at once, so adding 3 new frequencies to expand the range (e.g., 38 to 400 kHz) could greatly improve our ability to separate anatomically distinct groups of fish. New broadband acoustic technologies currently under development may also prove useful for taxonomic identification in the future [21, 22]. Physical sampling (e.g. via mid-water trawl) to validate acoustic data is difficult in the fast flows of the passage [9]. However, insight could be gained by sampling in lower flow areas east and west of the Passage and by drawing on local knowledge of the fish species present, their migration timing, and their behaviors [19].

The observed difference in fish density between ebb and flood tide could be the result of a number of factors. For example, asymmetric tidal flow could result in more fish being carried through the sampled location during the flood tide than the ebb tide. Alternately, fish could be utilizing the upper water column more during the ebb tide than the flood, but not observed in the AZFP data due to air entrainment backscatter in the top 10 m. Tidal differences in depth preference may be more common in migratory fish (for example, those displaying selective tidal stream transport [23-31]) than overwintering fish, but shouldn't be ruled out without more information from the upper portion of the water column. To better understand tidal differences in fish presence, more information is needed on the flow field and the horizontal distribution of fish in the passage during different tidal stages. There is also a need to develop better methods for processing and analyzing the portions of the water column affected by entrained air. Some headway has been made in separating out the entrained air backscatter using multiple frequencies and different mathematical approaches [11], and this is one avenue that should be explored at this site.

There was a clear diel change in vertical distribution of fish in the portion of water column examined (below the top 10 m which was excluded due to air entrainment). Fish were more evenly spread out in the water column at night. As water column backscatter did not decrease, this diel difference was unlikely due to fish moving upward into the excluded portion of the water column. Upward migration of fish at nightfall may have been evident in acoustic data collected at this site in June 2012 [32]. In the present study, however, the diel redistribution of fish was more likely related to the dissolution of schools at night, as schooling fish rely heavily on vision to remain aggregated [33, 34]. A similar pattern was seen at another tidal energy site [10], though fish density there was highest near the sea floor. Here, numerous dense aggregations of fish were visible in the middle and upper water column during the day but were not seen at night. This contributed to more variable water column fish density during the day. The majority of these fish were likely Atlantic herring [9, 18]. Herring is a schooling species, and their daily school dispersion and re-formation would generate a much more obvious diel change in vertical distribution than vertical movements of the less abundant species, like striped bass, which are known to migrate upward at night [3].

The presence of more fish higher in the water column at this site contrasts with observations of fish vertical distribution at a tidal energy site in Cobscook Bay, Maine, where fish densities were highest near the sea floor [10]. This disparity may be due to the different fish assemblages and/or local environmental factors (e.g., hydrodynamics, temperature, habitat types).

4.2 Fish at TISEC device depth

The proportion of fish backscatter at device depth (bottom 20 m) was found to differ with tidal stage but not with the diel stage, despite diel differences in vertical distribution. Unfortunately, backscatter cannot be easily changed to an absolute number or density of fish in a mixed fish assemblage without knowledge of the species of each individual fish or aggregation detected [13]. This is because the acoustic reflectivity of fish is largely determined by their anatomy (species, life stage, and size) and orientation within the acoustic beam [13]. If all fish are assumed to be the same species and size, the proportion of backscatter at device depth can be a direct estimate of the proportion of fish. In reality, this proportion must be scaled depending on the acoustic properties of the fish detected, but from this rough starting point it appears that a considerable proportion of fish within the region of the water column analysed was at device depth (32% during flood, 40% during ebb). The proportion would decrease if the uppermost 10 m of water could be included in analysis: near low slack water, an additional 10 m would more than double the amount of water above the TISEC device. A better method for dealing with entrained air needs to be investigated to allow, when possible, assessment of fish present in the upper 10 m of the water column.

4.3 Probability of spatial overlap

The vertical distributions presented here allowed the estimation of the probability that fish passing through the Minas Passage would spatially overlap with a TISEC device at the FORCE site. All three scenarios explored (uniform, ebb tide, and flood tide vertical distributions) yielded very low probabilities of spatial overlap — all less than 0.002 (0.2%) — which is not surprising given the width of the passage (5.5 km) and the comparably very small area spanned by a single TISEC device. Though the probabilities of spatial overlap were small, they did vary with tidal stage due to shifts in fish vertical distribution. This highlights the importance incorporating

actual data on fish use of a tidal energy site into predictions of device encounter, as well as the importance of considering depth of the device relative to that of the fish. At this site, more fish would be at TISEC device depth if the device under consideration were near the surface rather than bottom-mounted. Encounter probability will become more important in assessing device effects as deployments are scaled up from pilot-scale to commercial-scale arrays.

The horizontal distribution of fish at a tidal energy site must also be incorporated into encounter models. The spatial overlap probabilities estimated here assumed a uniform horizontal distribution of fish across the passage but, as with vertical distribution, the horizontal distribution of fish is likely to be non-uniform and dependent on the species present. For example, Atlantic sturgeon have been found to utilize the southern side of Minas Passage more than the northern side [35], whereas striped bass were more often detected mid-passage [19, 52]. Data on the horizontal distribution of fish would be best acquired via mobile hydroacoustic transects across the passage [32], and FORCE is currently working with University of Maine researchers to do so [36]. Results from the mobile surveys can later be combined with results presented here to build a better understanding of the likelihood that fish may encounter TISEC devices in Minas Passage.

It is important to recall that estimates of spatial overlap of fish with devices do not take into account the behavioural responses of fish to TISEC devices as they move through the passage. Though the distribution of different fish species and life stages will influence their likelihood of encountering tidal energy devices, fish sensory and locomotory abilities will influence if and how they physically interact. We have little reason to believe fish are passive particles in this environment, despite the strong currents. Elsewhere, there is evidence of fish responding to TISEC devices at a variety of spatial scales, from potential avoidance beginning as far as 140 m upstream [37] to evasion by even small fish (~10 cm) occurring within the nearest few meters [39, 40]. The sensory abilities of fish will affect at what distance they detect a TISEC device, and subsequently their likelihood for avoidance or evasion. Fish have a wide variety of senses to inform them of their environment, including vision, hearing, and the lateral line system [43-45], all of which are likely to be of use in avoiding TISEC devices and other obstacles [39]. The sensitivity of each sensory system varies with species and life stage [46] and can be modified by the environment—for example, striped bass may be less responsive to environmental cues at very low temperatures [19]. Assuming a fish detects a TISEC device, swimming power then becomes important for avoidance or evasion. Swimming power is proportional to fish length [47], and larger fish may be less likely to enter a turbine than smaller ones [39]. More observations of fish behaviour near TISEC devices (e.g. with split beam echosounders [37, 38], multibeam sonars [39, 40], or cameras if possible [41, 42]), as well as information on the perception and locomotion thresholds of different species and life stages of fish in loud, turbulent, high-speed environments, is necessary to better predict if fish will avoid or enter TISEC devices.

A future goal is to extend our probability of spatial overlap assessments and encounter probability models [53] to estimate probability of strike by turbine blades. Assuming a fish does not avoid a TISEC device upon encountering it, and instead enters the operating turbine, it then risks contact with turbine blades. Observing and quantifying strike in the field is likely to be incredibly difficult, if not impossible, primarily due to resolution limitations of acoustic equipment [39] and the difficulty of seeing in dark water by other means (e.g. video [48]).

However, laboratory simulations have found that fish tend to resist entering TISEC turbines even in confined spaces, with measured survival rates greater than 90% for those fish that do pass through [49, 50]. These studies have not examined survival rates in the dark, which may be an important factor in turbine blade evasion [39]. Also, conditions in laboratory flumes differ substantially from those in the field, e.g. with slower current speeds, less turbulent flow, and different acoustic environments. Given the limitations inherent in field observation techniques, there is a need for laboratory testing under more realistic conditions to better estimate survival rates of fish passing through TISEC devices, and to describe TISEC device cues that elicit responses in various species and life stages of fish. By combining such information with knowledge of the species present at tidal energy sites and their natural distribution and movements over various time scales, we can build a more complete picture of fish interactions with TISEC devices and better predict device effects on fish from individual to population levels.

4.4 AZFP performance

The AZFP performed well over the course of this deployment. There was no noticeable drift in sensitivity based on backscatter values of the surface. The signal to noise ratio was sufficiently high over the course of the collection period and did not change noticeably. The instrument was easy to install and the software was well-documented. We suggest duty cycling data collection so that echosounders like the AZFP do not ping simultaneously with other acoustic instruments, such as ADCPs, as the manual identification and removal of interference was time consuming. Duty cycling is also effective in reducing the amount of data stored to memory. Memory storage capacity and instrument battery life (if the sensor is not cabled) will define the maximum period of data collection. The duty cycling schedule should be determined based on what is known of the system (e.g., natural cycles likely to be present, such as the tidal cycle) to avoid introducing bias to results [38]. Additionally, the continuous dataset presented here can be subsampled to examine potential effects of duty cycling on results.

The AZFP is a single-beam system, and therefore is sufficient if relative metrics of density and distribution are all that are required. The utility of the data could be expanded if additional frequencies were added to the AZFP. The AZFP allows four single-beam transducers to be operated simultaneously; collecting data at a wide range of frequencies could help separate anatomically distinct groups of fish, potentially to species level [20, 21]. This will be necessary for predicting turbine effects on different fish populations.

5   Conclusion and recommendations

Fish were commonly observed throughout the period of data collection, from 8 December 2015 to 5 January 2016, and in fact density was higher during this period than the following June to July [15]. Many of these fish were likely Atlantic herring, and their consistent presence regardless of tidal or diel stage may indicate overwintering in the area, as suggested in [32]. The density and vertical distribution of fish varied with the environmental factors examined (tidal and diel stages). Future higher resolution temporal analyses will aid in understanding the cause of this variation.

The probabilities of spatial overlap that were estimated using device and passage areas combined with the vertical distribution of fish were all very small (less than 0.002), which is not surprising

for a single TISEC device in a large passage. Most of the fish present were in the upper portion of the water column analyzed (>20 m from the sea floor), with variation related to both tidal and diel stage. Integrating observations of the natural vertical distribution of fish (in contrast to a uniform vertical distribution) substantially reduced their likelihood of overlapping with a 20 m TISEC device fixed to the sea floor. The opposite would be true for a surface-deployed TISEC device. This highlights the importance of incorporating field observations of fish distribution into predictions of TISEC device effects.

The approach to modelling spatial overlap that was explored here does not take into account the distribution of different species over a given time period or behavior upon turbine encounter, which could result in device avoidance or evasion. The development of models on the effects of turbines on fish in Minas Passage should combine information on the natural vertical and horizontal distribution of fish within the passage with what is learned of encounter probability based on the tracking of tagged fish through the passage [19, 52, 53] and the responses to TISEC devices or other underwater obstacles in fast-flow environments.

The ASL AZFP worked very well for the month it was deployed, and provided some of the first long-term, high-resolution information on fish presence and vertical distribution at the FORCE tidal energy test site. Acoustic datasets like the one presented here have resolution and breadth that cannot be achieved by traditional physical sampling methods. Acoustic data are therefore invaluable for studying systems that change on a wide range of temporal scales (e.g. tidal to seasonal cycles). As a single beam system used in a mixed-species assemblage, the AZFP can provide relative indices of fish density and vertical distribution over time. If relative metrics are sufficient to answer the questions asked, this system is perfectly suitable for use at tidal energy sites.

In future deployments, we recommend the AZFP be duty-cycled to avoid simultaneous data collection with other acoustic instruments, such as the ADCP, to cut back on the necessary manual processing time. We also recommend expanding the frequency range of the AZFP through the addition of 3 transducers. Examining the frequency responses of detected fish (backscatter values across a range of frequencies) would improve our ability to separate anatomically distinct groups of fish. This and knowledge of which species are in the area during data collection periods may allow species identification. Physical sampling of fish (e.g. mid-water trawl) is difficult in the fast flows and complex bathymetry of the test site but could be safely conducted during slack water periods in adjacent waters where current speeds are lower. Insight on fish species' migration timing and behaviors could also be gained by drawing on local knowledge. We suggest incorporating more input from fishers and other knowledgeable community members into the interpretation of acoustic data. Improving our capacity to identify species within acoustic data will allow better predictions of TISEC device effects on different fish populations.

Entrained air extending from the surface continues to be a challenge for acoustic data collection and processing. In this case, it resulted in data analysis that completely omitted the upper 10 m of the water column for the four weeks of data collected. The effects of excluding portions of data contaminated by entrained air should be examined in future assessments of tidal energy sites; e.g., through simulation studies under a variety of assumptions of fish density within excluded regions. More information on the presence of fish within plumes of entrained air may

also be gathered via physical sampling of the uppermost water column, though this may be difficult at peak flows. In future work, it would be beneficial to explore methods of addressing entrained air signals in order to include as much of the upper 10 m as possible.

The fish assemblages of Minas Passage change substantially over the course of a year, with many seasonal species (some of which are commercially important, threatened, or endangered) migrating through at particular times. This report covers the collection and analysis of only one month of data, from early December to early January, but additional FAST platform deployments have since taken place in June-July 2016, June-July 2017, and September-October 2017. Additional deployments are planned through 2018, including December-January, April-May, June-July, and September-October. Analysis is underway on other AZFP data collected to date. These and future datasets will provide a more complete understanding of fish use of this site and their potential for interacting with TISEC devices.

6 Acknowledgements

7 References

[1]   R. Karsten, "Tidal energy resource assessment map for Nova Scotia," Acadia University, Wolfville, NS, Canada, Report prepared for OEER/OETR, November 2012.

[2]   O. Nakken, K. Olsen, "Target strength measurements of fish," Rap. Proces., vol. 170, pp. 52-69, 1977.

[3]   A. Bonanno, S. Goncharov, T. Knutsen, T. van der Meeren, L. Calise, E. Montella, A.R. Angotzi, A. Cuttitta, B. Patti, G. Basilone, G. Buscaino, J. Brunskog, S. Mazzola, "Experimental evaluation of target strength for herring larvae (*Clupea harengus*) at early developmental stages," in Proc. International Conference Underwater Acoustic Measurements: Technologies & Results, 2005.

[4]   V. Ermolchev, M. Zaferman, "Results of experiments on the video-acoustic estimation of fish target strength *in situ*," ICES Journal of Marine Science, vol. 60, pp. 544-547, 2003.

[5]   J.R. Nielsen, B. Lundgren, "Hydroacoustic *ex situ* target strength measurements on juvenile cod (*Gadus morhua* L.)," ICES J. Mar. Sci., vol. 56, pp. 627-639, 1999.

[6]   E. Ona, "Detailed *in situ* target strength measurements of O-group cod," ICES CM 1994/B, vol. 30, 9 p.p., 1994.

[7]   D. Chu, P.H. Wiebe, N.J. Copley, G.L. Lawson, V. Puvanendran, "Material properties of North Atlantic cod eggs and early-stage larvae and their influence on acoustic scattering," ICES J. Mar. Sci., vol. 60, pp. 508-515, 2003.

[8]   K.G. Foote, "Importance of the swimbladder in acoustic scattering by fish: a comparison of gadoid and mackerel target strengths. J. Acoust. Soc. Am., vol. 67(6), pp. 2084-2089, 1980.

[9]   G.D. Melvin, N.A. Cochrane, "Multibeam acoustic detection of fish and water column targets at high-flow sites," Estuar. Coast., vol. 38(suppl. 1), pp. S227-S240, 2015.

[10]   H. Viehman, G.B. Zydlewski, J. McCleave, and G. Staines, "Using acoustics to understand fish presence and vertical distribution in a tidally dynamic region targeted for energy extraction," Estuar. Coast., vol. 38(suppl. 1), pp. S215-S226, 2015.

[11]   S. Fraser, V. Nikora, B.J. Williamson, B.E. Scott, "Automatic active acoustic target detection in turbulent aquatic environments," Limnol. Oceanogr.-Meth., vol. 15, pp. 184-190, 2017.

[12]   K.G. Foote, "Linearity of fisheries acoustics, with addition theorems," J. Acoust. Soc. Am., vol. 73(6), pp. 1932-1940, 1983.

[13]   J. Simmonds and D.N. MacLennan, Fisheries acoustics: theory and practice, Oxford: Blackwell, 2005.

[14]   M. Baker, M. Reed, A.M. Redden, "Temporal Patterns in Minas Basin Intertidal Weir Fish Catches and Presence of Harbour Porpoise during April – August 2013," Report to the Fundy Ocean Research Centre for Energy, ACER Technical Report 120, 2014.

[15]   H. Viehman, T. Boucher, A.M. Redden, "Winter and summer differences in probability of fish encounter (spatial overlap) with MHK devices," in Proc. European Wave and Tidal Energy Conference, 2017.

[16]   I. Solberg and S. Kaartvedt, "Surfacing behavior and gas release of the physostome sprat (*Sprattus sprattus*) in ice-free and ice-covered waters," Mar. Biol., vol. 161, pp. 285-296, 2014.

[17]   B. Wilson, R.S. Batty, L.M. Dill, "Pacific and Atlantic herring produce burst pulse sounds," Proc. R. Soc. Lond. B, vol. 271(suppl.), pp. S95-S97, 2004.

[18]   M.J. Dadswell, "Occurrence and migration of fishes in Minas Passage and their potential for tidal turbine interaction," BioIdentification Associates, Report prepared for Fundy Ocean Research Centre for Energy, 2010.

[19]   F.M. Keyser, J.E. Broome, R.G. Bradford, B. Sanderson, and A.M. Redden, "Winter presence and temperature-related diel vertical migration of Striped Bass (*Morone saxatili*s) in an extreme high flow site in Minas Passage, Bay of Fundy," Can. J. Fish. Aquat. Sci., vol. 73(12), pp. 1777-1786, 2016.

[20]   R.J. Korneliussen and E. Ona, "Verified acoustic identification of Atlantic mackerel," ICES CM2004, paper R20, 14 pp., 2004.

[21]   J.K. Horne, "Acoustic approaches to remote species identification: a review," Fish Oceanogr., vol. 9(4), pp. 356-371, 2000.

[22]   D.A. Demer, L.N. Andersen, C. Bassett, L. Berger, D. Chu, J. Condiotty, G.R. Cutter et al., "2016 USA–Norway EK80 Workshop Report: Evaluation of a wideband echosounder for fisheries and marine ecosystem science," ICES Coop. Res. Rep., no. 336, 69 pp., 2017, available at http://doi.org/10.17895/ices.pub.2318.

[23]   J.D. McCleave, R.C. Kleckner, "Selective tidal stream transport in the estuarine migration of glass eels of the American eel (*Anguilla rostrata*)," J. Cons. Int. Explor. Mer., vol. 40, pp. 262-271, 1982.

[24]   J.J. Dodson and W.C. Leggett, "Behavior of adult American shad (*Alosa sapidissima*) homing to the Connecticut River from Long Island Sound," J. Fish. R. Board Can., vol. 30, pp. 1847-1860, 1973.

[25]   G.P. Arnold, M. Greer Walker, L.S. Emerson, B.H. Holford, "Movements of cod (*Gadus morhua* L.) in relation to the tidal streams in the southern North Sea," ICES J. Mar. Sci., vol. 51, pp. 207-232, 1994.

[26]   D.A. Levy and A.D. Cadenhead, "Selective tidal stream transport of adult sockeye salmon (*Oncorhynchus nerka*) in the Fraser River Estuary, Can. J. Fish. Aquat. Sci., vol. 52, pp. 1-12, 1995.

[27]   A. Moore, M. Ives, M. Scott, S. Bamber, "The migratory behavior of wild sea trout (*Salmo trutta* L.) smolts in the estuary of the River Conwy, North Wales," Aquaculture, vol. 198, pp. 57-68, 1998.

[28]   J.F. de Veen, "On selective tidal transport in the migration of North Sea Plaice (*Pleuronectes platessa*) and other flatfish species," Netherlands J. Sea Res., vol. 12(2), pp. 115-147, 1978.

[29]   M. Greer Walker, F.R. Harden Jones, G.P. Arnold, "The movements of plaice (*Pleuronectes platessa* L.) tracked in the open sea," J. Cons. Int. Explor. Mer., vol. 38(1), pp. 58-86, 1978.

[30]   M. Castonguay, D. Gilbert, "Effects of tidal streams on migrating Atlantic mackerel, *Scomber scombrus* L.," ICES J. Mar. Sci. vol. 52(6), pp. 941-954, 1995.

[31]   K.N. Lacoste, J. Munro, M. Castonguay, F.J. Saucier, J.A. Gagné, "The influence of tidal streams on the pre-spawning movements of Atlantic herring, *Clupea harengus* L., in the St Lawrence estuary," ICES J. Mar. Sci., vol. 58, pp.1286-1298, 2001.

[32]   G.D. Melvin, N.A. Cochrane, "Investigation of the vertical distribution, movement and abundance of fish in the vicinity of proposed tidal power energy conversion devices,"

Final report to the Offshore Energy Research Association, OEER/OETR Research Project 300-170-09-12, 2014.

[33] C.W. Glass, C.S. Wardle, W.R. Mojsiewicz, "A light intensity threshold for schooling in the Atlantic mackerel, *Scomber scombrus*," J. Fish. Biol., vol. 29(suppl. A), pp. 71-81, 1986.

[34] L.A.F. Nilsson, U.H. Thygesen, B. Lundgren, B.F. Nielsen, J.R. Nielsen, J.E. Beyer, "Vertical migration and dispersion of sprat (*Sprattus sprattus*) and herring (*Clupea harengu*s) schools at dusk in the Baltic Sea," Aquat. Living Resour., vol. 16, pp. 317-324, 2003.

[35] M.J.W. Stokesbury, L.M. Logan-Chesney, M.F. McLean, C.F. Buhariwalla, A.M. Redden, J.W. Beardsall, J.E. Broome, M.J. Dadswell, "Atlantic sturgeon and temporal distribution in Minas Passage, Nova Scotia, Canada, a region of future tidal energy extraction," PLoS ONE, vol. 11(7), e0158387, 2017.

[36] Fundy Ocean Research Center for Energy, "Environmental effects monitoring program quarterly report: January 1-March 31, 2017," available at http://fundyforce.ca/environment/monitoring.

[37] H. Shen, G.B. Zydlewski, H.A. Viehman, G. Staines, "Estimating the probability of fish encountering a marine hydrokinetic device," Renew. Energy, vol. 97, pp. 746-756, 2016.

[38] H.A. Viehman, "Hydroacoustic analysis of the effects of a tidal power turbine on fishes," dissertation, University of Maine, Orono, ME, Dec. 2016.

[39] H. Viehman, G.B. Zydlewski, "Fish interaction with a commercial-scale tidal energy device in a field setting," Estuaries Coast., vol. 38(suppl. 1), pp. S241-S252, 2015.

[40] M. Bevelhimer, C. Scherelis, J. Colby, M.A. Adonizio, "Hydroacoustic assessment of behavioral responses by fish passing near an operating tidal turbine in the East River, New York," Trans. Am. Fish. Soc., vol. 146(5), pp. 1028-1042, 2017.

[41] L. Hammar, S. Andersson, L. Eggertsen, J. Haglund, M. Gullström, Jimmy Ehnberg, Sverker Molander, "Hydrokinetic turbine effects on fish swimming behavior," PLoS ONE, vol. 8(12), e84141, 2013.

[42] M. Broadhurst, S. Barr, C.D.L. Orme, "In-situ ecological interactions with a deployed tidal energy device: an observational pilot study," Ocean Coast. Manage., vol. 99, pp. 31-38, 2014.

[43] A.N. Popper and C.R. Schilt, "Hearing and acoustic behavior (basic and applied)," in J.F. Webb, R.R. Fay, A.N. Popper, editors. Fish Bioacoustics, New York: Springer Science+Business Media, pp. 17-48, 2008.

[44] H. Bleckmann and R. Zelick, "Lateral line system of fish," Int. Zool., vol. 4, pp. 13-25, 2009.

[45]   D.H. Evans, editor, The physiology of fishes, Boca Raton: CRC Press, 1993.

[46]   J.H.S. Blaxter, "Development of sense organs and behavior of teleost larvae with special reference to feeding and predator avoidance," T. Am. Fish. Soc., vol. 115(1), pp. 98-114, 1986.

[47]   F.W.H. Beamish, "Swimming capacity," in W.S. Hoar, D.J. Randal, editors, Fish Physiology, Volume VII: Locomotion, New York: Academic Press, pp.101-187, 1978.

[48]   A. Avila, R. Hull, S. Matzner, G. Staines, C. Trostle, G.E.L. Harker-Klimeš, "Triton: Igiugig video analysis," Pacific Northwest National Laboratory, Richland, WA, Report prepared for the U.S. Department of Energy contract DE-AC05-76RL01830, September 2016.

[49]   S.V. Amaral, M.S. Bevelhimer, G.F. Čada, D.J. Giza, P.T. Jacobson, B.J. McMahon, B.M. Pracheil, "Evaluation of behavior and survival of fish exposed to an axial-flow hydrokinetic turbine," N. M. J. Fish. Manage., vol. 35(1), pp. 97-113, 2015.

[50]   T. Castro-Santos, A. Haro, "Survival and behavioral effects of exposure to a hydrokinetic turbine on juvenile Atlantic salmon and adult American shad," Estuar. Coast., vol. 38(suppl 1), pp. S203-S214, 2015.

[51]   H.A. Viehman and G.B. Zydlewski, "Multi-scale temporal patterns in fish presence in a high-velocity tidal channel," PLoS ONE, accepted.

[52]   A.M. Redden, M.J.W. Stokesbury, J. Broome, F. Keyser, J. Gibson, E. Halfyard, M. McLean, R. Bradford, M. Dadswell, B. Sanderson and R. Karsten, "Acoustic tracking of fish movements in the Minas Passage and FORCE Demonstration Area: Pre-turbine Baseline Studies (2011-2013)", Report to the Fundy Ocean Research Centre for Energy and the Offshore Energy Research Association. ACER Technical Report 118, 153 pp. Acadia University, Wolfville, NS, Canada, 2014.

[53]   B. Sanderson, A.M. Redden, "Use of fish tracking data to model striped bass turbine encounter probability in Minas Passage", Final Report to the Offshore Energy Research Association of Nova Scotia. ACER Technical Report No. 122, 54 pp, Acadia University, Wolfville, NS, Canada, 2016.